JCTC Journal of Chemical Theory and Computation

Coarse Graining of Intermolecular Vibrations by a Karhunen-Loève Transformation of Atomic Displacement Vectors

Hirohiko Houjou*

Institute of Industrial Science, University of Tokyo, 4-6-1 Komaba, Meguro-ku, Tokyo 153-8505, Japan

Received April 9, 2009

Abstract: We have formulated a procedure for evaluating the anisotropic stiffness of a molecular assembly. First, we show how to reduce the dimensions of the matrices that appear in a conventional Hessian analysis of mass-weighted coordination by using a 12-dimensional transverse-rotational basis set for expansion. This treatment yields matrix representations of the intermolecular force and inertial load of the constituent molecules. Next we applied this procedure to 2-aminopyridine dimers and numerically analyzed the low-frequency (∼THz region) normal-mode vibrations. By validating the elements of stiffness matrix, this study exemplifies a derivation of the parameters necessary for the normal-mode analysis of a large system like a crystal, without any explicit representation of the potential functions.

1. Introduction

The increasing interest in supramolecular materials and biomolecular systems demands better fundamental understanding of intermolecular interactions. Recently, terahertz (THz) spectroscopy has been used for direct observation of intermolecular interactions in such contexts as the analysis of the hydration of sugars, the arrangement of nucleobases in DNA, and the polymorphism of medicinal drugs.[1−5] The terahertz region (∼300 GHz to 3 THz) covers hydrogen bond vibrations, van der Waals interactions, overall molecular distortion, and molecular libration; hence, the comparison of theoretical and experimental vibrational spectra can provide a molecular-level picture of the macroscopic phenomena of materials. Accordingly, several quantum chemical and molecular mechanics-based approaches have been reported.[6−12] In addition, anharmonic effects should also be included to quantitatively explain experimental results.[13,14]

Because we have reached the primary stage of interpreting the contents of THz spectra, it seems important to clarify the harmonic behavior of a molecular system in which intermolecular forces dominate the optimum arrangement of the molecules in a material. Various phenomena related to intermolecular vibrations and librations have been studied by Hessian-based methods such as normal-mode analyses and lattice dynamics (phonon band calculations).[15−18] In applications of these methods to macromolecular systems, coarse graining of molecular representation has frequently been employed as an approach toward reducing computational consumption.[15c,d,19] Combined with empirical force field parameters, the coarse graining approach has been successful to some extent in reproducing the collective motions of proteins, which resonate at GHz frequencies. In these studies, the elements of the dynamical matrix were evaluated as second derivatives of a potential function whose composition included Lennard-Jones-type repulsion-dispersion and electrostatic interactions; hence, the results depend on the force field parameters used. The efforts in developing the force field seem to be devoted to constructing a set of universal parameters by decomposing the molecular interactions into components for respective atom−atom or multipole−multipole pairs.[20−23] For these efforts to succeed, some intrinsic difficulties need to be dealt with, for example, the balancing of several types of potential depth and the incorporation of secondary (cooperative) effects such as instantaneous induced polarization.

On the one hand, on the basis of the above points, it may be insufficient to apply an empirical force field to a Hessian-

* Corresponding author phone: +81(3)5452-6367; fax: +81(3)5452-6366; e-mail: houjou@iis.u-tokyo.ac.jp.

10.1021/ct900169f CCC: $40.75
Published on Web 05/29/2009

based analysis of THz spectra, in which specific intermolecular interactions are sensitively reflected. On the other hand, some groups satisfactorily reproduced THz spectra by normal-mode calculation based on ab initio molecular orbital or density functional theory methods.[7−12] However, applying these quantum chemical methods to such large systems as proteins, nucleotides, and molecular crystals is obviously difficult in view of the consumption of computational time and resources. In this study based on ab initio quantum chemical calculations, we attempt to derive the elements of a dynamical matrix for a coarse-grained representation of a molecular assembly. The normal-mode frequency calculated by the quantum chemical method reflects the curvature of the potential surface, into which the electronic effects are adequately incorporated. Because the intermolecular forces are responsible for the low-frequency vibrations, it seems quite reasonable to extract meaningful parameters from the huge amount of numerical atomic displacement data. The thus-obtained "tailor-made" parameters will lead to reliable predictions of THz spectra.

2. Theoretical Basis

In the framework of Hessian analysis of molecular vibration, the displacement vectors $\mathbf{X}$ are obtained by diagonalizing the mass-weighted Hessian matrix ($\mathbf{M}^{-1/2}\mathbf{K}\mathbf{M}^{-1/2}$) with the eigenvalue matrix $\mathbf{\Omega}$ that contains the corresponding frequency ω as follows[24]

$$(\mathbf{M}^{-1/2}\mathbf{K}\mathbf{M}^{-1/2})(\mathbf{M}^{1/2}\mathbf{X}) = (\mathbf{M}^{1/2}\mathbf{X})\mathbf{\Omega}^2 \tag{1}$$

For an isolated single molecule, the dimension of $\mathbf{M}$ and $\mathbf{K}$ is $3N$, where N is the number of constituent atoms, and the diagonalization gives six zero-eigenvalues for the molecular motions of pure translation and pure rotation. For a system composed of two molecules that have N_{I} and N_{II} atoms, respectively, the number of degrees of internal freedom is $3(N_{\mathrm{I}} + N_{\mathrm{II}}) - 6$, in which $3N_{\mathrm{I}} - 6$ and $3N_{\mathrm{II}} - 6$ modes of motion originate from the internal freedom of the respective molecule. Consequently, six residual modes are attributed to the degrees of freedom of the intermolecular vibration.

In practical normal-mode analysis for dimeric systems, the vibrations of intermolecular motions appear within a wavenumber range of 10−200 cm^{-1}, clearly separate from the wavenumber ranges of intramolecular motions that appear in the region of 400−4000 cm^{-1}. This observation suggests that there are only small coupling effects among the intermolecular and intramolecular vibrations. Therefore, the atomic displacement of an intermolecular vibration is approximately represented by a combination of several basic motions of a "frozen" molecule. The intermolecular vibrational motions are approximately represented by a linear combination of the translational and rotational (hereafter denoted as T/R) motions of the constituent molecules as a basis set. For example, the basis for symmetric transverse motion along the x-axis is hereafter denoted as $\mathrm{T}_x + \mathrm{T}_x$ (Figure 1). This representation is a kind of Karhunen-Loève (KL) expansion, a method for extracting the principal components of poly dimensional vectors.[25] In the space

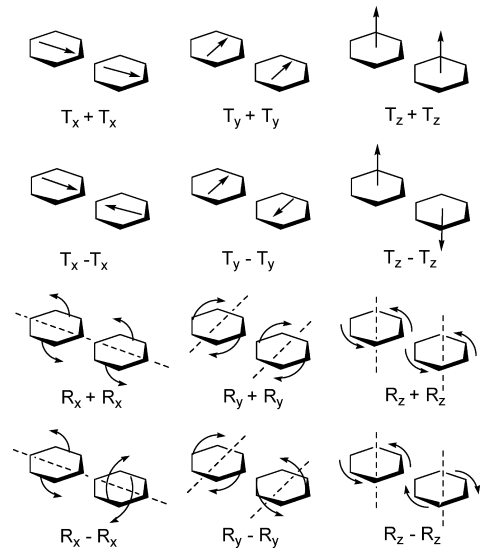

Figure 1. Schematic representation of the twelve basic motions of a molecular dimer.

spanned by the six basic motions each of molecules I and II, Hessian analysis results in six nonzero eigenvalues for intermolecular vibration modes and six zero-eigenvalues for pure translation and pure rotation of a given dimeric system.

The vectors that represent the basic motions of the monomer are normalized as follows

$$(\mathbf{T}_x\,\mathbf{T}_y\,\mathbf{T}_z) = \frac{1}{\sqrt{N}}\begin{pmatrix} 1 & 0 & 0 \\ 0 & 1 & 0 \\ 0 & 0 & 1 \\ \vdots & \vdots & \vdots \\ 1 & 0 & 0 \\ 0 & 1 & 0 \\ 0 & 0 & 1 \end{pmatrix} \tag{2}$$

$$(\mathbf{R}_x\,\mathbf{R}_y\,\mathbf{R}_z) = \begin{pmatrix} 0 & z_1\sin\theta_y & -y_1\sin\theta_z \\ -z_1\sin\theta_x & 0 & x_1\sin\theta_z \\ y_1\sin\theta_x & -x_1\sin\theta_y & 0 \\ \vdots & \vdots & \vdots \\ 0 & z_N\sin\theta_y & -y_N\sin\theta_z \\ -z_N\sin\theta_x & 0 & x_N\sin\theta_z \\ y_N\sin\theta_x & -x_N\sin\theta_y & 0 \end{pmatrix} \tag{3a}$$

$$\theta_q = \sin^{-1}\left(\sqrt{\sum_{i=1}^{N}(r_i^2 - q_i^2)}\right)^{-1} \quad q = \{x, y, z\} \tag{3b}$$

$$r_i^2 = x_i^2 + y_i^2 + z_i^2 \tag{3c}$$

where $\mathbf{T}_q$ and $\mathbf{R}_q$ ($q = x, y, z$) are column vectors of dimension $3N$, and (x_n, y_n, z_n) is the position of the n-th atom with respect to the center of mass. Thus, the $3(N_{\mathrm{I}} + N_{\mathrm{II}}) \times 12$ matrix $\mathbf{B}$ for the KL transformation of a dimeric system is written as follows, in which, e.g., $\bar{\mathbf{T}}_x$ represents $-\mathbf{T}_x$, and subscripts I and II denote the monomers I and II

$$\mathbf{B} = \frac{1}{\sqrt{2}}\begin{pmatrix} \mathbf{T}_{\mathrm{I}x}\mathbf{T}_{\mathrm{I}y}\mathbf{T}_{\mathrm{I}z}\mathbf{R}_{\mathrm{I}x}\mathbf{R}_{\mathrm{I}y}\mathbf{R}_{\mathrm{I}z} & \mathbf{T}_{\mathrm{I}x}\mathbf{T}_{\mathrm{I}y}\mathbf{T}_{\mathrm{I}z}\mathbf{R}_{\mathrm{I}x}\mathbf{R}_{\mathrm{I}y}\bar{\mathbf{R}}_{\mathrm{I}z} \\ \mathbf{T}_{\mathrm{II}x}\mathbf{T}_{\mathrm{II}y}\mathbf{T}_{\mathrm{II}z}\mathbf{R}_{\mathrm{II}x}\mathbf{R}_{\mathrm{II}y}\mathbf{R}_{\mathrm{II}z} & \bar{\mathbf{T}}_{\mathrm{II}x}\bar{\mathbf{T}}_{\mathrm{II}y}\bar{\mathbf{T}}_{\mathrm{II}z}\bar{\mathbf{R}}_{\mathrm{II}x}\bar{\mathbf{R}}_{\mathrm{II}y}\bar{\mathbf{R}}_{\mathrm{II}z} \end{pmatrix} \tag{4}$$

The orthogonality of the column vectors in the mass-weighted T/R basis $\mathbf{M}^{1/2}\mathbf{B}$ depends on the selection of the

coordinate system. These vectors can be modified to $\mathbf{M}^{1/2}\mathbf{C}$ so as to be orthonormal by using $\mathbf{S}$, the overlap matrix $\mathbf{B}^t\mathbf{M}\mathbf{B}$

$$\mathbf{M}^{1/2}\mathbf{C} = \mathbf{M}^{1/2}\mathbf{B}\mathbf{S}^{-1/2} \tag{5a}$$

$$\mathbf{S} = \mathbf{B}^t\mathbf{M}\mathbf{B} \tag{5b}$$

Here we redefine $\mathbf{X}$ as a $3(N_\mathrm{I} + N_\mathrm{II}) \times 12$ matrix that contains the atomic displacement vectors for six transverse (columns 1−3) and rotational motions (columns 4−6) and six intermolecular vibration modes (columns 7−12) of the dimer. Then, the coefficients of the KL expansion are collected in $\mathbf{\Xi}$, a 12×12 matrix. In other words, the displacement vectors of dimension $3N$ are reduced to 12 dimensions

$$\mathbf{\Xi} = \mathbf{C}^t\mathbf{M}\mathbf{X} \tag{6}$$

According to the definition of $\mathbf{S}$, we can construct a matrix $\mathbf{\Gamma}^{-1}$ that represents the inertial load of the molecules

$$\begin{aligned}\mathbf{\Gamma}^{-1} &\equiv \mathbf{N}^{1/2}\mathbf{S}\mathbf{N}^{1/2} \\ &= \mathbf{N}^{1/2}\mathbf{S}^{1/2}\mathbf{C}^t\mathbf{M}\mathbf{C}\mathbf{S}^{1/2}\mathbf{N}^{1/2} \\ &= \frac{1}{2}\begin{pmatrix} (M_\mathrm{I}+M_\mathrm{II})\mathbf{E} & 0 & (M_\mathrm{I}-M_\mathrm{II})\mathbf{E} & 0 \\ 0 & \mathbf{I}_\mathrm{I}+\mathbf{I}_\mathrm{II} & 0 & \mathbf{I}_\mathrm{I}-\mathbf{I}_\mathrm{II} \\ (M_\mathrm{I}-M_\mathrm{II})\mathbf{E} & 0 & (M_\mathrm{I}+M_\mathrm{II})\mathbf{E} & 0 \\ 0 & \mathbf{I}_\mathrm{I}-\mathbf{I}_\mathrm{II} & 0 & \mathbf{I}_\mathrm{I}+\mathbf{I}_\mathrm{II} \end{pmatrix}\end{aligned} \tag{7}$$

where M and $\mathbf{I}$ are the molecular weight and the tensor of inertia, respectively, of a monomer. In eq 7, we define the matrix $\mathbf{N}^{-1}$ as consisting of the molecular weights and the spatial extent of atoms of given monomers (θ_q^{-2}/N nearly equals the variance of the atomic location around the q-axis)

$$\mathbf{N}^{-1} = \frac{1}{2}\begin{pmatrix} (N_\mathrm{I}^1+N_\mathrm{II}^1)\mathbf{E} & 0 & (N_\mathrm{I}^1-N_\mathrm{II}^1)\mathbf{E} & 0 \\ 0 & \mathbf{\Theta}_\mathrm{I}^2+\mathbf{\Theta}_\mathrm{II}^2 & 0 & \mathbf{\Theta}_\mathrm{I}^2-\mathbf{\Theta}_\mathrm{II}^2 \\ (N_\mathrm{I}^1-N_\mathrm{II}^1)\mathbf{E} & 0 & (N_\mathrm{I}^1+N_\mathrm{II}^1)\mathbf{E} & 0 \\ 0 & \mathbf{\Theta}_\mathrm{I}^2-\mathbf{\Theta}_\mathrm{II}^2 & 0 & \mathbf{\Theta}_\mathrm{I}^2+\mathbf{\Theta}_\mathrm{II}^2 \end{pmatrix} \tag{8a}$$

$$\mathbf{E} = \begin{pmatrix} 1 & 0 & 0 \\ 0 & 1 & 0 \\ 0 & 0 & 1 \end{pmatrix}, \mathbf{\Theta} = \begin{pmatrix} \theta_x & 0 & 0 \\ 0 & \theta_y & 0 \\ 0 & 0 & \theta_z \end{pmatrix} \tag{8b}$$

The matrix $\mathbf{\Gamma}$, named by analogy with the G-matrix in the GF method,[24] represents the measure of inertia in a given internal coordinate system. Similarly a matrix $\mathbf{\Phi}$ can be defined to represent a measure of stiffness

$$\mathbf{\Phi} = \mathbf{N}^{1/2}\mathbf{S}^{1/2}\mathbf{C}^t\mathbf{K}\mathbf{C}\mathbf{S}^{1/2}\mathbf{N}^{1/2} \tag{9}$$

Using eqs 6, 7, and 9, we can rewrite eq 1 into the following equations

$$(\mathbf{\Gamma}^{1/2}\mathbf{\Phi}\mathbf{\Gamma}^{1/2})\mathbf{L} = \mathbf{L}\mathbf{\Omega}^2 \tag{10a}$$

$$\mathbf{L} = \mathbf{\Gamma}^{-1/2}\mathbf{N}^{-1/2}\mathbf{S}^{-1/2}\mathbf{\Xi} \tag{10b}$$

Because the matrix $\mathbf{\Gamma}^{-1/2}\mathbf{\Phi}\mathbf{\Gamma}^{-1/2}$ is Hermitian, its eigenvectors $\boldsymbol{L}_i$ (i-th column vectors of $\mathbf{L}$) have to be orthogonal but not necessarily normalized. The product $\mathbf{L}^t\mathbf{L}$ gives a diagonal matrix $\mathbf{\Lambda}^2$, the elements of which represent the modal masses in the reduced T/R coordinate system

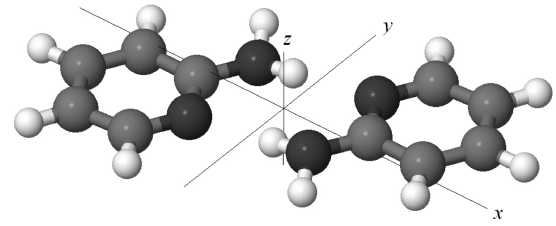

Figure 2. Coordinate system used for analysis of the intermolecular vibrations of 2-aminopyridine dimer.

$$\begin{aligned}\mathbf{\Lambda}^2 &= \mathbf{L}^t\mathbf{L} \\ &= \mathbf{\Xi}^t\mathbf{C}^t\mathbf{M}\mathbf{C}\mathbf{\Xi} \\ &= \mathbf{X}^t\mathbf{M}\mathbf{X}.\end{aligned} \tag{11}$$

Equation 11 indicates that the modal masses in the T/R coordinate system would ideally be identical to those in the full-atom coordinate system, if $\mathbf{M}^{-1/2}\mathbf{C}$ provides a sufficiently good basis of the expansion (*vide infra*). In the present study, however, we redefine $\mathbf{\Lambda}^2$ by collecting the squared norms (λ_i^2) of $\boldsymbol{L}_i$ as diagonal elements

$$\mathbf{\Lambda}^2 \equiv \begin{pmatrix} \lambda_1^2 & & & 0 \\ & \lambda_2^2 & & \\ & & \ddots & \\ 0 & & & \lambda_{12}^2 \end{pmatrix} . \tag{12}$$

Using $\mathbf{\Lambda}^{-1}$ as the normalization factor, we can obtain $\mathbf{U}$, which is approximately unitary (and could be unitary if the basis set of KL expansion is complete). The squared components of $\mathbf{U}$ represent the mixing ratio of the basic motions like $\mathrm{T}_x + \mathrm{T}_x$ in a given atomic displacement for intermolecular vibration

$$\mathbf{U} = \mathbf{\Gamma}^{-1/2}\mathbf{N}^{-1/2}\mathbf{S}^{-1/2}\mathbf{\Xi}\mathbf{\Lambda}^{-1} \tag{13}$$

Then, we can obtain the force constant matrix $\mathbf{\Phi}$ for a given internal T/R coordinate system as follows

$$\mathbf{\Phi} = \mathbf{\Gamma}^{-1/2}\mathbf{U}\mathbf{\Omega}^2\mathbf{U}^t\mathbf{\Gamma}^{-1/2} \tag{14}$$

3. Computational Details

Hydrogen-bonded dimers of 2-aminopyridine and its 5-halogenated derivatives were selected as examples for the analysis described above. The geometry of the dimers was optimized by means of the Hartree−Fock method using the 6-311G** basis set, and the structure thus obtained was used for the normal-mode vibration analysis at the same level of calculation. These molecular orbital calculations were performed with the Gaussian03W program.[26] The values of the geometry and eigenvectors were picked up from the output file and then processed with versatile spreadsheet software.

4. Results and Discussion

4.1. Derivation of Force Constants. For the optimized structure of a dimer of 2-aminopyridine, we set the coordinate system as shown in Figure 2. The values of the Cartesian coordinates were used for preparing the $\mathbf{B}$ and $\mathbf{C}$ matrices.

Table 1. Elements (in g mol^{-1} unit) of $\mathbf{\Gamma}^{-1}$

	T_x	T_y	T_z	R_x	R_y	R_z
T_x	94.1	0.00	0.00	0.00	−0.00	−0.00
T_y	0.00	94.1	0.00	−0.00	−0.00	0.00
T_z	0.00	0.00	94.1	0.00	0.00	0.00
R_x	0.00	−0.00	0.00	156.6	42.9	0.69
R_y	−0.00	−0.00	0.00	42.9	111.3	−1.29
R_z	−0.00	0.00	0.00	0.69	−1.29	267.7

Table 2. Comparison of the Modal Mass and Modal Stiffness Calculated for Internal Coordinate Systems

	ν (cm^{-1})	ω^2/N_A (s^{-2} mol)	modal mass (g mol^{-1})		modal stiffness (N m^{-1})	
			T/R	full-atom	T/R	full-atom
Twist	16.5	16.0	4.03	4.11	0.06	0.07
Buckle	28.4	47.7	4.73	4.71	0.23	0.22
Opening	63.6	238.9	4.29	4.36	1.02	1.04
Staggered	67.7	270.7	6.20	6.30	1.68	1.70
Shear	77.4	353.7	6.21	6.27	2.20	2.21
Stretch	109.4	706.0	5.68	5.70	4.01	4.02

The first six columns (for transverse and rotational motions) of **X** were made by a procedure similar to that used to make the **B** matrix, and the subsequent six columns were picked up from the output of the calculation of normal-mode vibration. Then we obtained **Ξ** according to eq 6. The 12 × 12 diagonal matrix **Ω** was made from the six eigenvalues (converted to ω^2/N_A in s^{-2} mol unit) of the normal-mode analysis. The first six elements (for transverse and rotational motions) were forced to be zero, and the latter six elements were allocated for the intermolecular vibrations.

Next, following eq 7, we constructed the $\mathbf{\Gamma}^{-1}$ matrix, which contains information on the inertial load (Table 1). Because we are studying a homodimer, only the top-left quarter of the matrix is fundamental (i.e., the full matrix is a direct sum of this table). The block related to transverse motions, i.e., T_x, T_y, and T_z, is diagonal, and the elements Γ_{ii}^{-1} substantially coincide with the molecular weight (in g mol^{-1}) of the monomer. The block related to rotational motions, i.e., R_x, R_y, and R_z, represents the tensor of inertia given in units of g Å^2 mol^{-1} (= 10^{-23} kg m^2 mol^{-1}). Then we derived $\mathbf{\Gamma}^{-1/2}$, which was used to make **L**.

By visualizing the atomic displacement, we labeled each vibration mode by one of six nicknames (Twist, Buckle, Staggered, Opening, Shear, and Stretch) that represent the character of the motion.[27] The modal mass (λ^2/g mol^{-1}) of each vibration mode for the internal T/R basis is given in Table 2. These values are in fairly good agreement within a factor of 0.98−1.00 with the modal mass calculated for the full-atom coordinate. This agreement was as expected from eq 12, which also validates the completeness of the T/R basis set. Accordingly, we can also see good agreement between the values of the modal stiffness that were calculated for respective coordinate systems.

By following eq 13, we obtained **U**. Columns 7−12 of **U** are shown in Table 3. We confirmed that the product of $\mathbf{U}^t$ and **U** approximates a unit matrix, again showing that the T/R motions that were used serve as a good basis for expansion of the intermolecular vibration.

Table 3. Elements of the Block of Intermolecular Vibrations in **U** Matrix

	Twist	Buckle	Opening	Staggered	Shear	Stretch
$T_x + T_x$	−0.005	0.005	−0.009	0.000	0.000	0.000
$T_y + T_y$	0.001	−0.001	0.008	0.000	0.000	0.000
$T_z + T_z$	−0.003	−0.009	−0.006	0.000	0.000	0.000
$R_x + R_x$	0.000	0.000	0.000	−0.095	−0.010	0.117
$R_y + R_y$	0.000	0.000	0.000	−0.680	−0.620	0.040
$R_z + R_z$	0.000	0.000	0.000	−0.201	0.312	0.772
$T_x - T_x$	0.000	0.000	0.000	0.594	−0.556	0.529
$T_y - T_y$	0.000	0.000	0.000	−0.299	0.344	0.321
$T_z - T_z$	0.000	0.000	0.000	0.215	0.301	−0.080
$R_x - R_x$	−0.959	0.192	−0.180	0.000	0.000	0.000
$R_y - R_y$	0.201	0.981	0.056	0.000	0.000	0.000
$R_z - R_z$	0.200	0.012	−0.982	0.000	0.000	0.000

Table 4. Elements (in N m^{-1}) of **Φ** in the *Gerade* Block

	A_g-like			B_g-like		
	$T_x - T_x$	$T_y - T_y$	$R_z + R_z$	$R_x + R_x$	$R_y + R_y$	$T_z - T_z$
$T_x - T_x$	37.9	0.37	30.9	4.20	3.24	−5.11
$T_y - T_y$	0.37	13.1	36.3	3.83	−0.64	0.11
$R_z + R_z$	30.9	36.3	124.8	13.7	−0.06	−3.42
$R_x + R_x$	4.20	3.83	13.7	3.92	8.40	−3.55
$R_y + R_y$	3.24	−0.64	−0.06	8.40	29.2	−11.1
$T_z - T_z$	−5.11	0.11	−3.42	−3.55	−11.1	4.60

Table 5. Elements (in N m^{-1}) of **Φ** in the *Ungerade* Block

	B_u-like			A_u-like		
	$T_x + T_x$	$T_y + T_y$	$R_z - R_z$	$R_x - R_x$	$R_y - R_y$	$T_z + T_z$
$T_x + T_x$	0.00	0.00	0.34	0.06	0.02	0.00
$T_y + T_y$	0.00	0.00	−0.29	−0.04	0.00	0.00
$R_z - R_z$	0.34	−0.29	61.89	7.67	−1.05	0.21
$R_x - R_x$	0.06	−0.04	7.67	4.07	1.93	0.01
$R_y - R_y$	0.02	0.00	−1.05	1.93	5.33	−0.05
$T_z + T_z$	0.00	0.00	0.21	0.01	−0.05	0.00

It can be seen from Table 2 that for the vibration modes of Twist, Buckle, and Opening, the atomic displacements are predominantly represented by $R_x - R_x$ (92%), $R_y - R_y$ (96%), and $R_z - R_z$ (96%) motions, respectively. Although we assigned the vibration modes at 67.7 and 77.4 cm^{-1} as Staggered and Shear motions, it is hard to distinguish one from the other by observing the visualized motion. These two modes are represented as combinations of $R_y + R_y$ and $T_x - T_x$ but with a difference in their mixing phase. The Stretch motion, which is often treated by a simple pseudodiatomic approximation, is actually dominated by $R_z + R_z$ (60%) motion for this case.

Subsequently, we obtained the **Φ** matrix according to eq 14. Tables 4 and 5 summarize the elements of **Φ** in the *gerade* block and the *ungerade* block, respectively, where the elements (Φ_{ij}) are given in units of N m^{-1}. For the terms related to rotational motions, the values correspond to a torque measured in N m^{-1} Å^2 (= 10^{-20} N m). Because the molecular system belongs to the C_i point group, the off-diagonal elements of **Φ** between the motions of the *gerade* representation ($T_x - T_x$, $T_y - T_y$, $T_z - T_z$, $R_x + R_x$, $R_y + R_y$, and $R_z + R_z$) and the motions of the *ungerade* representation ($T_x + T_x$, $T_y + T_y$, $T_z + T_z$, $R_x - R_x$, $R_y - R_y$, and $R_z - R_z$) are definitely zero. Furthermore, if we neglect the pyramidization of the amino groups, the molec-

Table 6. Comparison of Force Constants and Wavenumbers of Basic Motions

	wavenumber (cm^{-1})		force constant (N m^{-1})	
	T/R basis	rigid body	T/R basis	rigid body
$T_x - T_x$	82.6	90.9	18.9	22.9
$T_y - T_y$	48.5	53.0	6.5	9.6
$T_z - T_z$	28.8	29.4	2.3	2.4
$R_x + R_x$	20.6	18.5	2.0	1.6
$R_y + R_y$	66.7	30.9	14.6	3.1
$R_z + R_z$	88.9	18.4	62.4	2.7
$R_x - R_x$	21.0	26.1	2.0	3.1
$R_y - R_y$	28.5	0.0	2.7	0.0
$R_z - R_z$	62.6	61.9	30.9	30.2

ular dimer has nearly C_{2h} symmetry. Thus, dividing the table into blocks for the A_g-like motions ($T_x - T_x$, $T_y - T_y$, and $R_z + R_z$) and the B_g-like motions ($R_x + R_x$, $R_y + R_y$, and $T_z - T_z$) is informative. For the A_g vs A_g and B_g vs B_g blocks, the diagonal elements show relatively large positive values, but some off-diagonal elements are as large as the diagonal ones. The off-diagonal elements in the A_g vs B_g block are relatively small but are not quite zero, suggesting a mixing of the A_g and B_g representations due to the deformation from a strict C_{2h} symmetry. In particular, the cross term (13.7 N m^{-1}) between $R_x + R_x$ and $R_z + R_z$ is exceptionally large. For the B_u vs B_u and A_u vs A_u blocks, the diagonal terms of $T_x + T_x$, $T_y + T_y$, and $T_z + T_z$ are naturally close to zero, because these bases represent the transverse motion of the molecular dimer. The off-diagonal terms in the A_u vs B_u block are relatively small, but again we observe an exceptionally large coupling constant (7.67 N m^{-1}) between $R_x - R_x$ and $R_z - R_z$.

4.2. Comparison with the Rigid Body Approximation. In a previous study, we investigated the mechanical nature of multiply hydrogen-bonded systems by means of ab initio quantum chemical calculations.[28] By a multivariate analysis of the curvature of the potential surface for 20 dimeric molecular systems, we derived a set of force constants for translational shear in the x, y, and z directions. The force constants only roughly reproduced the frequencies of the intermolecular vibration modes of a molecular dimer, which in turn indicated the significance of the off-diagonal terms of the dynamical matrix when evaluating the frequency of intermolecular vibration. In the present study, we succeeded in explicitly obtaining the full elements of the stiffness matrix for an internal coordinate system reduced by KL transformation. Here we attempt to compare the present results with those of our previous calculations. If we neglect the off-diagonal terms, we can calculate the wavenumber for each mode of the basic motions as follows

$$\tilde{\nu}_i = \frac{1}{2\pi c}\sqrt{\frac{\Phi_{ii}}{\Gamma_{ii}}} \qquad (15)$$

Table 6 lists the wavenumbers calculated with eq 15. The values (in cm^{-1}) for $R_x - R_x$ (21.0), $R_y - R_y$ (28.5), and $R_z - R_z$ (62.6) motions are in good agreement with those for Twist (16.5), Buckle (28.4), and Opening (63.6) motions, respectively, as expected from the predominant component of these normal modes (Table 3). The wavenumbers for $T_x - T_x$ (82.6), $T_y - T_y$ (48.5), $R_y + R_y$ (66.7), and $R_z + R_z$ (88.9) are within a range similar to those of Shear (67.7), Stagger (77.4), and Stretch (109.4) modes but are not exactly identical. We interpret this mismatch in frequencies as a result of appreciable coupling terms, namely, $T_x - T_x$ vs $R_z + R_z$ (30.9 N m^{-1}) and $T_y - T_y$ vs $R_z + R_z$ (36.3 N m^{-1}), as given in Table 4.

On the other hand, based on simple rigid body mechanics, the wavenumber of homodimeric molecule is given as follows

$$\tilde{\nu}_i = \frac{1}{2\pi c}\sqrt{\frac{(M_{\mathrm{I}} + M_{\mathrm{II}})K_i}{M_{\mathrm{I}}M_{\mathrm{II}}}} = \frac{1}{2\pi c}\sqrt{\frac{2K_i}{M}} \qquad (16)$$

where K_i (i denotes the type of motion) is the force constant of the intermolecular interaction, and M ($= M_{\mathrm{I}} = M_{\mathrm{II}}$) is either the molecular weight (for transverse motion) or moment of inertia divided by 1 $Å^2$ (for rotational motion). Therefore, we can compare a series of force constants for 12 basic motions by simply calculating $\Phi_{ii}/2$. Table 6 compares the force constants and wavenumbers calculated by means of the method described in this paper (eq 15) and those calculated by rigid body mechanics (eq 16). For the rigid body mechanical calculation, we used a set of force constants that we developed for NH···N hydrogen bonds.[28] Note that for transverse motion (e.g., $T_x - T_x$), the force constants (18.9, 6.5, 2.3 N m^{-1}) derived from the T/R based expansion are in good agreement with those (22.9, 9.6, 2.4 N m^{-1}) from a rigid body approximation. As for rotational motions, the force constants for antisymmetric combinations (e.g., $R_x - R_x$) show good agreement between the two methods. A deviation found in the $R_y - R_y$ mode may be attributed to the intentional neglect of the pyramidization of the amino group in our former work. On the contrary, a similar comparison for symmetric combinations (e.g., $R_x + R_x$) shows a considerable disagreement between the results obtained by means of the two methods. This disagreement demonstrates the difficulty in deriving force constants analytically for molecules with complicated shapes.

4.3. Effects of Molecular Inertial Load on Frequency. Among the various intermolecular vibration modes, Stretch motion is of special interest because of its spectroscopic accessibility as well as its relevance to the strongest force of intermolecular interaction.[29−31] Conventionally, the relation between the frequency and force constants is analyzed based on the pseudodiatomic approximation or on its modified formulation. Although the latter method is applicable to asymmetric top dimers, it can handle only the force constant of stretching motion.[29] As demonstrated above, however, the frequency of the Stretch mode is determined as a result of coupling among $T_x - T_x$, $T_y - T_y$, and $R_z + R_z$ motions, all of which belong to the A_g representation on the assumption that the dimer has C_{2h} symmetry. These three basic motions give rise to two other motions with A_g representation, that is, Shear mode vibrations and rotation of the dimer around the z-axis (R_z). Our present study provides a comprehensive interpretation of the relation between the frequency and force constants of intermolecular vibration.

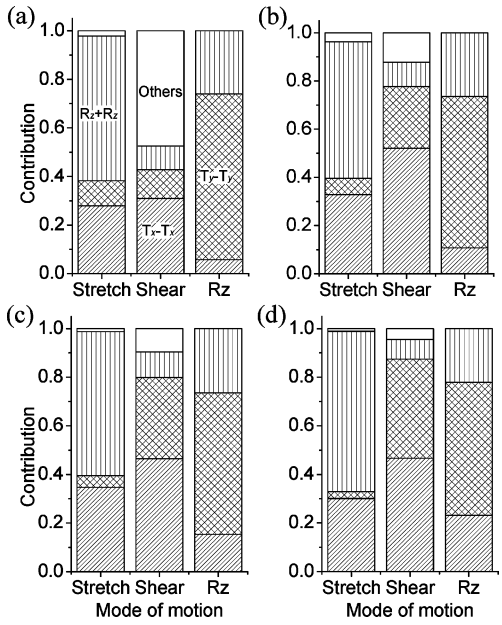

Figure 3. Contributions of $T_x - T_x$, $T_y - T_y$, and $R_z + R_z$ motions to the vibration modes of (a) 2-aminopyridine and (b) 5-fluoro-, (c) 5-chloro-, and (d) 5-bromo-2-aminopyridines.

Previously, we pointed out that the frequencies of the intermolecular vibration modes of 5-halogenated-2-aminopyridine do not follow the pseudodiatomic model.[28] For example, the frequency of the Stretch mode was nearly insensitive to changes in the molecular weight. Here we attempt to clarify the relation between the frequencies and molecular weight of 2-aminopyridines on the basis of our present formulation. Figure 3(a)-(d) shows the contribution (U_{ij}^2) of the $T_x - T_x$, $T_y - T_y$, and $R_z + R_z$ motions to Stretch and Shear mode vibrations and R_z motion, for 2-aminopyridine and its 5-halogenated derivatives. As can be seen from these figures, each of these motions is sufficiently described as a combination of three basic motions with A_g representation, although their contributions differ slightly depending on the molecule. This result suggests that the frequency of the Stretch and Shear modes can be approximately evaluated by diagonalizing the 3×3 partial matrix of $\mathbf{\Gamma}^{1/2}\mathbf{\Phi}\mathbf{\Gamma}^{1/2}$ that corresponds to the cross terms among the $T_x - T_x$, $T_y - T_y$, and $R_z + R_z$ bases.

Figure 4 shows the values of selected elements in the stiffness matrix $\mathbf{\Phi}$ as a function of $(M_0/M)^{1/2}$, where M_0 and M are the molecular weights of 2-aminopyridine and 5-halogenated-2-aminopyridine, respectively. The diagonal elements related to transverse displacement, namely, $\Phi_{Tx\text{-}Tx,Tx\text{-}Tx}$ and $\Phi_{Ty\text{-}Ty,Ty\text{-}Ty}$ (Figure 3(a)), are scarcely influenced by substitution at the 5-position, and their cross term $\Phi_{Tx\text{-}Tx,Ty\text{-}Ty}$ (Figure 3(b)) is nearly equal to zero. These results indicate that the restoring force along the *x*- and *y*-axes mainly originates in double NH···N hydrogen bonds, and any effects from halogen substitution are negligibly small. As for $\Phi_{Rz+Rz,Rz+Rz}$, the force constant for the twisting distortion, the value steeply increases with increasing molecular weight. Because $\Phi_{Rz+Rz,Rz+Rz}$ is proportional to the torque around the *z*-axis, this constant should increase with the square of distance (R_{HB}) between the center of mass and the centers of hydrogen bonding sites.[32] Figure 4(a) shows the

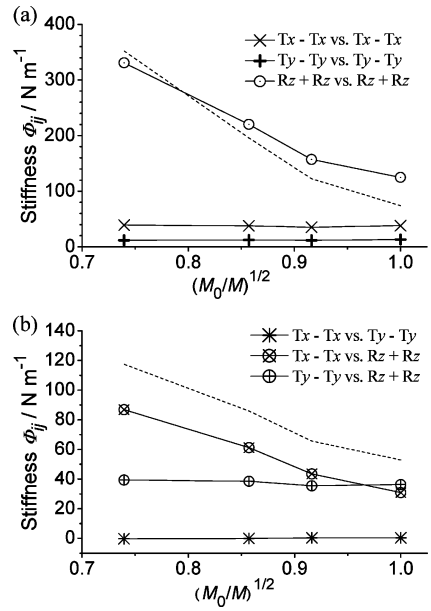

Figure 4. (a) Diagonal and (b) off-diagonal elements of the stiffness matrix ($\mathbf{\Phi}$) as functions of $(M_0/M)^{-1/2}$. Dashed lines indicate the values of $\Phi_{Tx\text{-}Tx,Tx\text{-}Tx}R_{HB}^2$ (in (a)) and $\Phi_{Tx\text{-}Tx,Tx\text{-}Tx}R_{HB}$ (in (b)) for comparison with a model based on rigid mechanics.

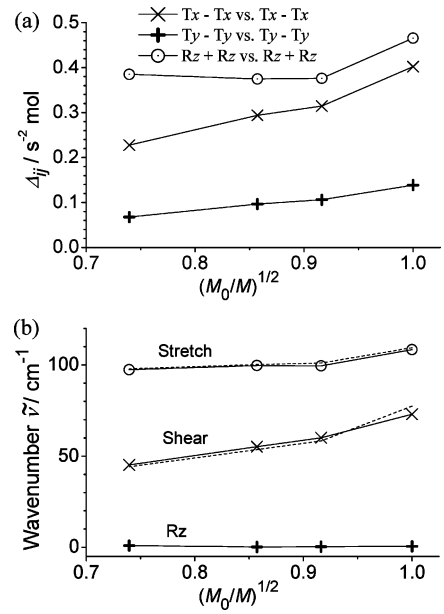

Figure 5. (a) The diagonal elements and (b) the eigenvalues of a 3×3 partial matrix of $\mathbf{\Delta}$. The frequencies of the Stretch and Shear modes calculated for the full-atomic representation are also imposed on (b).

plot of $\Phi_{Tx\text{-}Tx,Tx\text{-}Tx}R_{HB}^2$, which is in fairly good agreement with $\Phi_{Rz+Rz,Rz+Rz}$, again suggesting that hydrogen bonding is a predominant interaction for intermolecular forces. Similarly, the plot of $\Phi_{Tx\text{-}Tx,Tx\text{-}Tx}R_{HB}$ shows behavior parallel to that of $\Phi_{Tx\text{-}Tx,Rz+Rz}$.

Figure 5(a) shows some elements of $\mathbf{\Gamma}^{1/2}\mathbf{\Phi}\mathbf{\Gamma}^{1/2}$ ($\equiv \mathbf{\Delta}$), a dynamical matrix for a given T/R coordinate. The elements related to transverse motion, namely, $\Delta_{Tx\text{-}Tx,Tx\text{-}Tx}$ and $\Delta_{Ty\text{-}Ty,Ty\text{-}Ty}$, are nearly proportional to $(M_0/M)^{1/2}$, which is a result expected from the pseudodiatomic model. The behavior

of the value of $\Delta_{Rz+Rz,Rz+Rz}$ is not simple, but it is rather insensitive to the change of molecular weight. This constancy is interpretable from the compensation of the changes in $\Phi_{Rz+Rz,Rz+Rz}$ and $\Gamma^{-1}{}_{Rz+Rz,Rz+Rz}$, both of which are roughly proportional to $R_{HB}{}^2$. Figure 5(b) shows the eigenvalues of a 3×3 matrix that contains the elements related to $T_x - T_x$, $T_y - T_y$, and $R_z + R_z$ in $\mathbf{\Delta}$. One of the eigenvalues nearly equals zero, suggesting its correspondence to R_z motion. The other two eigenvalues are in excellent agreement with those of the Stretch and Shear modes that were calculated by using full-atom coordination. Consequently, the apparent complicated behavior of the Stretch mode frequency observed for the 5-halogenated-2-aminopyridine dimer is a result of the constant stiffness ($\sim$20 N m^{-1}) of double NH$\cdots$N hydrogen bonds and the sequential transfer of the center of mass. This result clearly shows that our approach is useful for understanding the fundamentals of intermolecular vibrations even for asymmetric top dimers with various moments of inertia.

5. Conclusions

This report presents a procedure to evaluate the elements of the stiffness matrix relevant to intermolecular force based on normal-mode calculations for full-atomic representation. We utilized a variation of Karhunen-Loève transformation that is quite useful for extracting the characteristics of serial data such as digitalized information. We developed a quantitative representation for characterizing atomic displacement during intermolecular vibration, which had conventionally been classified according to visualization of molecular motion. By using a compressed 12-dimensional space of molecular motion, we obtained the elements of the stiffness matrix, which yields a dynamical matrix when combined with the inertial load of the molecules in question. Note also that the treatment based on KL transformation is not confined to a rigid molecule approximation. It would be possible to take into account the mixing of intra- and intermolecular vibrations in the THz region by adding some eigenvectors for the single molecular normal mode to the basis set of the KL expansion. Accordingly, the method presented in this study is quite versatile for evaluating the parameters necessary for the coarse-grained normal-mode calculation of a large molecular assembly including a periodic system as well as for obtaining deep insight into the nature of intermolecular vibration.

References

(1) For recent review: Plusquellic, D. F.; Siegrist, K.; Heilweil, E. J.; Esenturk, O. *Chem. Phys. Chem.* **2007**, *8*, 2412–2431.

(2) Heyden, M.; Bründermann, E.; Heugen, U.; Niehues, G.; Leitner, D. M.; Havenith, M. *J. Am. Chem. Soc.* **2008**, *130*, 5773–5779.

(3) Fischer, B. M.; Walther, M.; Jepsen, P. U. *Phys. Med. Biol.* **2002**, *47*, 3807–3814.

(4) Taday, P. F.; Bradley, I. V.; Arnone, D. D.; Pepper, M. *J. Pharm. Sci.* **2003**, *92*, 831–838.

(5) Aaltonen, J.; Allesø, M.; Mirza, S.; Koradia, V.; Gordon, K. C.; Rantanen, J. *Eur. J. Pharm. Biopharm.* **2009**, *71*, 23–37.

(6) Day, G. M.; Zeitler, J. A.; Jones, W.; Rades, T.; Taday, P. F. *J. Phys. Chem. B* **2006**, *110*, 447–456.

(7) Takahashi, M.; Ishikawa, Y.; Nishizawa, J.; Ito, H. *Chem. Phys. Lett.* **2005**, *401*, 475–482.

(8) Rungsawang, R.; Ueno, Y.; Tomita, I.; Ajito, K. *J. Phys. Chem. B* **2006**, *110*, 21259–21263.

(9) Jepsen, P. U.; Clark, S. J. *Chem. Phys. Lett.* **2007**, *442*, 275–280.

(10) (a) Siegrist, K.; Bucher, R.; Mandelbaum, I.; Walker, A. R. H.; Balu, R.; Gregurick, S. K.; Plusquellic, D. F. *J. Am. Chem. Soc.* **2006**, *128*, 5764–5775. (b) Zhang, H.; Siegrist, K.; Plusquelic, D. F.; Gregurick, S. K. *J. Am. Chem. Soc.* **2008**, *130*, 17846–17857. (c) Zhang, H.; Zukowski, E.; Balu, R.; Gregurick, S. K. *J. Mol. Graphics Modell.* **2009**, *27*, 655–663.

(11) Saito, S.; Inerbaev, T. M.; Mizuseki, H.; Igarashi, N.; Note, R.; Kawazoe, Y. *Chem. Phys. Lett.* **2006**, *423*, 439–444.

(12) (a) Fedor, A. M.; Korter, T. M. *Chem. Phys. Lett.* **2006**, *429*, 405–409. (b) Korter, T. M.; Balu, R.; Campbell, M. B.; Beard, M. C.; Gregurick, S. K.; Heilweil, E. J. *Chem. Phys. Lett.* **2006**, *418*, 65–70. (c) Allis, D. G.; Fedor, A. M.; Korter, T. M.; Bjarnason, J. E.; Brown, E. R. *Chem. Phys. Lett.* **2007**, *440*, 203–209. (ca) Allis, D. G.; Korter, T. M. *Chem. Phys. Chem.* **2006**, *7*, 2398–2408. (d) Allis, D. G.; Prokhorova, D. A.; Korter, T. M. *J. Phys. Chem. A* **2006**, *110*, 1951–1959.

(13) Brauer, B.; Gerber, R. B.; Kabelác, M.; Hobza, P.; Bakker, J. M.; Riziq, A. G. A.; de Vries, M. S. *J. Phys. Chem. A* **2005**, *109*, 6974–6984.

(14) Špirko, V.; Šponer, J.; Hobza, P. *J. Chem. Phys.* **1997**, *106*, 1472–1479.

(15) For examples: (a) Ma, J. *Structure* **2005**, *13*, 373–380. (b) Bahar, I.; Rader, A. J. *Curr. Opin. Struct. Biol.* **2005**, *15*, 586–592. (c) Li, G.; Cui, Q. *Biophys. J.* **2004**, *86*, 743–763. (d) Li, G.; Cui, Q. *Biophys. J.* **2002**, *83*, 2457–2474. (e) Kindt, J. T.; Schmuttenmaer, C. A. *J. Chem. Phys.* **1997**, *106*, 4389–4400.

(16) Dove, M. T. In *Introduction to Lattice Dynamics*; Cambridge University Press: New York, 1993.

(17) (a) Neto, N.; Righini, R.; Califano, S.; Walmsley, S. H. *Chem. Phys.* **1978**, *29*, 167–179. (b) Schettino, V.; Califano, S. *J. Mol. Struct.* **1983**, *100*, 459–483.

(18) Kearley, G. J.; Johnson, M. R.; Tomkinson, J. *J. Chem. Phys.* **2006**, *124*, 044514.

(19) (a) Durand, D.; Trinquier, G.; Sanejourand, Y.-H. *Biophys. J.* **1994**, *34*, 759–771. (b) Tama, F.; Gadea, F. X.; Marques, O.; Sanejourand, Y.-H. *Prot. Struct. Funct. Gen.* **2000**, *41*, 1–7.

(20) Willock, D. J.; Price, S. L.; Leslie, M.; Catlow, C. R. A. *J. Comput. Chem.* **1995**, *16*, 628–647.

(21) (a) Weiner, S. J.; Kollman, P. A.; Case, D. A.; Singh, U. C.; Ghio, C.; Alagona, G.; Profeta, S.; Weiner, P. *J. Am. Chem. Soc.* **1984**, *106*, 765. (b) Cornell, W. D.; Cieplak, P.; Bayly, C. I.; Gould, I. R.; Merz, K. M., Jr.; Ferguson, D. M.; Spellmeyer, D. C.; Fox, T.; Caldwell, J. W.; Kollman, P. A. *J. Am. Chem. Soc.* **1995**, *117*, 5179–5197.

(22) MacKerell, A. D.; Wiórkiewicz-Kuczera, J.; Karplus, M. *J. Am. Chem. Soc.* **1995**, *117*, 11946–11975.

(23) Sun, H. *J. Phys. Chem. B* **1998**, *102*, 7338–7364.

(24) Wilson, E. B.,Jr.; Decius, J. C.; Cross, P. C. In Molecular Vibrations, Dover Publications, Inc.: New York, 1980.

(25) Ryckelynck, D.; Chinesta, F.; Cueto, E.; Ammar, A. *Arch. Comput. Meth. Engng.* **2006**, *13*, 91–128.

(26) Frisch, M. J.; Trucks, G. W.; Schlegel, H. B.; Scuseria, G. E.; Robb, M. A.; Cheeseman, J. R.; Montgomery, J. A., Jr.; Vreven, T.; Kudin, K. N.; Burant, J. C.; Millam, J. M;. Iyengar, S. S.; Tomasi, J.; Barone, V.; Mennucci, B.; Cossi, M.; Scalmani, G.; Rega, N.; Petersson, G. A.; Nakatsuji, H.; Hada, M.; Ehara, M.; Toyota, K.; Fukuda, R.; Hasegawa, J.; Ishida, M.; Nakajima, T.; Honda, Y.; Kitao, O.; Nakai, H.; Klene, M.; Li, X.; Knox, J. E.; Hratchian, H. P.; Cross, J. B.; Adamo, C.; Jaramillo, J.; Gomperts, R.; Stratmann, E.; Yazyev, O.; Austin, A. J.; Cammi, R.; Pomelli, C.; Ochterski, J. W.; Ayala, P. Y.; Morokuma, K.; Voth, G. A.; Salvador, P.; Dannenberg, J. J.; Zakrzewski, V. G.; Dapprich, S.; Daniels, A. D.; Strain, M. C.; Farkas, O.; Malick, D. K.; Rabuck, A. D.; Raghavachari, K.; Foresman, J. B.; Ortiz, J. V.; Cui, Q.; Baboul, A. G.; Clifford, S.; Cioslowski, J.; Stefanov, B. B.; Liu, G.; Liashenko, A.; Piskorz, P.; Komaromi, I.; Martin, R. L.; Fox, D. J.; Keith, T.; Al-Laham, M. A.; Peng, C. Y.; Nanayakkara, A.; Challacombe, M.; Gill, P. M. W.; Johnson, B.; Chen, W.; Wong, M. W.; Gonzalez, C.; Pople, J. A. *Gaussian 03, Revision C.02*; Gaussian, Inc.: Wallingford, CT, 2004.

(27) Diekmann, S. *EMBO J.* **1989**, *8*, 1–4.

(28) Houjou, H.; Koga, R. *J. Phys. Chem. A* **2008**, *112*, 11256–11262.

(29) (a) Legon, A. C.; Millen, D. J. *Chem. Rev.* **1986**, *86*, 635–657. (b) Legon, A. C.; Millen, D. J. *Acc. Chem. Res.* **1987**, *20*, 39–46. (c) Millen, D. J. *Can. J. Chem.* **1985**, *63*, 1477–1479.

(30) (a) Müller, A.; Talbot, F.; Leutwyler, S. *J. Chem. Phys.* **2000**, *112*, 3717–3725. (b) Müller, A.; Talbot, F.; Leutwyler, S. *J. Chem. Phys.* **2002**, *116*, 2836–2847. (c) Müller, A.; Talbot, F.; Leutwyler, S. *J. Am. Chem. Soc.* **2002**, *124*, 14486–14494. (d) Müller, A.; Talbot, F.; Leutwyler, S. *J. Chem. Phys.* **2001**, *115*, 5192–5202.

(31) Melandri, S.; Sanz, M. E.; Caminati, W.; Favero, P. G.; Kisiel, Z. *J. Am. Chem. Soc.* **1998**, *120*, 11504–11509.

(32) This simple model assumes the potential function of $V(x, \theta) = (1/2)\Phi_{Tx\text{-}Tx}(x + R_{HB}\theta)^2$. The second derivatives are given as $\partial^2V/\partial\theta^2 = \Phi_{Tx\text{-}Tx}R_{HB}^2$ and $\partial^2V/\partial x\partial\theta = \Phi_{Tx\text{-}Tx}R_{HB}$.

CT900169F